Acta Pharmaceutica Sinica B 2021;11(11):3527−3541

Chinese Pharmaceutical Association
Institute of Materia Medica, Chinese Academy of Medical Sciences

Acta Pharmaceutica Sinica B

www.elsevier.com/locate/apsb
www.sciencedirect.com

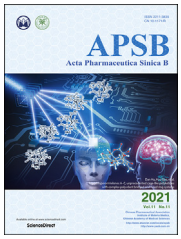

ORIGINAL ARTICLE

Integrative lipidomic and transcriptomic study unravels the therapeutic effects of saikosaponins A and D on non-alcoholic fatty liver disease

Xiaojiaoyang Li[a,†], Junde Ge[b,c,†], Yajing Li[a], Yajie Cai[a], Qi Zheng[a], Nana Huang[b], Yiqing Gu[a], Qi Han[a], Yunqian Li[a], Rong Sun[b,c,*], Runping Liu[a,*]

[a]*Beijing University of Chinese Medicine, Beijing 100029, China*
[b]*The Second Hospital of Shandong University, Shandong University, Ji'nan 250033, China*
[c]*Advanced Medical Research Institute, Shandong University, Ji'nan 250012, China*

Received 22 December 2020; received in revised form 3 February 2021; accepted 9 February 2021

KEY WORDS

Saikosaponin;
Nonalcoholic fatty liver disease;
Lipidome;
Transcriptome;
Lipid metabolism

Abstract Nonalcoholic fatty liver disease (NAFLD) has become one of the most prominent causes of chronic liver diseases and malignancies. However, few therapy has been approved. Radix Bupleuri (RB) is the most frequently used herbal medicine for the treatment of liver diseases. In the current study, we aim to systemically evaluate the therapeutic effects of saikosaponin A (SSa) and saikosaponin D (SSd), the major bioactive monomers in RB, against NAFLD and to investigate the underlying mechanisms. Our results demonstrated that both SSa and SSd improved diet-induced NAFLD. Integrative lipidomic and transcriptomic analysis revealed that SSa and SSd modulated glycerolipid metabolism by regulating related genes, like *Lipe* and *Lipg*. SSd profoundly suppressed the fatty acid biosynthesis by downregulating *Fasn* and *Acaca* expression and promoted fatty acid degradation by inducing *Acox1* and *Cpt1a* expression. Bioinformatic analysis further predicted the implication of master transcription factors, including peroxisome proliferator-activated receptor alpha (PPARα), in the protective effects of SSa and SSd. These results were further confirmed *in vitro* in mouse primary hepatocytes. In summary, our study uncoded the complicated mechanisms underlying the promising anti-steatosis activities of saikosaponins (SSs), and provided critical evidence inspiring the discovery of innovative therapies based on SSa and SSd for the treatment of NAFLD and related complications.

*Corresponding authors. Tel./fax: +86 10 53912122.
E-mail addresses: sunrong@sdu.edu.cn (Rong Sun), liurunping@bucm.edu.cn (Runping Liu).
[†]These authors made equal contributions to this work.
Peer review under responsibility of Chinese Pharmaceutical Association and Institute of Materia Medica, Chinese Academy of Medical Sciences.

https://doi.org/10.1016/j.apsb.2021.03.018

1. Introduction

Nonalcoholic fatty liver disease (NAFLD) is now quickly becoming one of the most prominent causes of chronic liver disorders and constitutes a major risk factor of liver malignancy worldwide. Already today, its prevalence ranges between 20% and 30% in the general population with an still rising incidence[1,2]. Nonalcoholic fatty liver (NAFL) is characterized by hepatic steatosis (excessive cytoplasmatic accumulation of lipids in hepatocytes), representing the early stage of NAFLD, and is usually associated with other metabolic syndromes, including obesity, type-2 diabetes, and cardiometabolic conditions[3]. From a mechanistic perspective, the excessive fat deposition in NAFL is mainly attributed to the disruption of hepatic lipid metabolism homeostasis, including increased lipid uptake and biosynthesis, and decreased lipid degradation. Accumulated free fatty acid-mediated lipotoxicity and overloading of mitochondrial capacity concurrently contribute to the activation of multiple cell stress pathways, including but not limited to oxidative stress and endoplasmic reticulum stress. Immune responses and proinflammatory environment following stress-mediated apoptosis further aggravates lipotoxicity-related hepatocellular injury and triggers the deposition of the extracellular matrix (ECM)[4]. With these above increase of hepatocellular injury and emergence of necrotizing inflammatory responses, NAFL potentially and uncontrollably develops into the more severe stage, nonalcoholic steatohepatitis (NASH)[5]. The continuum of liver abnormalities may further progress to liver fibrosis and cirrhosis, and eventually hepatic malignancies.

Although NAFLD is of increasing concern since it is highly prevalent, potentially aggressive, and progressing, no therapy has been approved. Targeting intrahepatic lipid accumulation is considered as the primary therapeutic strategy for NAFLD[6]. The peroxisome proliferator-activated receptors (PPARs), including PPARα, β/δ, and γ, are a family of nuclear receptors that have been well-characterized to be master regulators in lipid transport, fatty acid oxidation, and inflammation[7]. Among them, PPARα is predominantly expressed in the liver and is closely related to hepatic fatty acid metabolism[8]. PPARα transcriptionally activates the expression of fatty acid transportation-related genes to facilitate the uptake and trafficking of long-chain fatty acids in the liver and also promotes the expression of genes involved in fatty acid catabolism. Acyl-coenzyme A oxidase 1 (ACOX1), primary enzymes responsible for the shortening of very-long-chain fatty acid (VLCFA), carnitine palmitoyl-transferase 1α (CPT-1α), which is essential for the initiation of fatty acid β-oxidation, and acyl-coenzyme A (CoA) dehydrogenase family (ACADs), which directly catalyzes the degradation of fatty acids, are all established as downstream targets of PPARα activation[9]. Compelling evidence implicated that PPARα contributed to the homeostasis between lipogenesis, ketone bodies production, and cholesterol metabolism by regulating 3-hydroxy-3-methylglutaryl (HMG)-CoA synthase 2 and malonyl-CoA decarboxylase. Next-generation PPARα or pan-PPARs agonists, such as pioglitazone, elafibranor, and saroglitazar, have been suggested to induce the resolution of NASH in clinical trials[10–12]. However, due to striking and severe adverse impacts, including weight gain, peripheral edema, bone fractures, and even congestive heart failure, several previous PPAR agonist medications have been withdrawn from the market, and the safety of next-generation PPARs agonism medications yet to be extensively evaluated prior to the U.S. Food and Drug Administration (FDA) approvement. Recently, targeting the bile acid-farnesoid X receptor (FXR) axis has become a novel approach for the treatment of NAFLD. Emerging studies demonstrated that the activation of intrahepatic FXR suppressed lipogenesis and alleviated steatosis in the liver by reducing bile acid secretion and also directly regulating lipid metabolism-related genes. A synthetic FXR agonist obeticholic acid has achieved the milestone of clinical trials[13,14]. Interestingly, interruption of bile acid enterohepatic cycle by inhibiting apical sodium-dependent bile acid transporter (ASBT) in the ileum significantly reduced the bile acid pool, improved serum cholesterol/low-density lipoprotein (LDL) homeostasis, and reversed the hepatic lipid accumulation in both experimental animal models and NAFLD patients[15]. However, the phase II clinical trial of SHP626 (Volixibat), the only ASBT inhibitor that gained FDA fast track, was terminated probably due to severe diarrhea, which was not confirmed by its developer, Shire Pharmaceuticals Ltd. (Dublin, Ireland). Collectively, the discovery and development of novel therapeutic options for NAFLD are urgently required.

NAFLD is a complicated disease associated with the dysregulation of multiple and cross-talking biological pathways as described above. However, current scientific strategies for discovering treatment against NAFLD are usually focusing on a single target. Hence, identifying and evaluating bioactive components derived from classic formulas in traditional Chinese medicine (TCM) with promising hepatoprotective effects are potentially efficient and safe approaches for the discovery of novel therapies for NAFLD, since TCM is considered to be multi-targeting and has been clinically used for thousands of years[16]. Radix Bupleuri (RB) is the dry root of *Bupleurum chinense* DC. (Apiaceae) and *Bupleurum scorzoneri-folium* Willd., and has been widely used in TCM for over 2000 years. Clinically, RB is the principal herbal product presented in almost all TCM formulas used for the treatment of various liver diseases, including but not limited to fatty liver, chronic or viral hepatitis, cirrhosis, and even hepatocellular carcinoma[17]. Modern phytochemistry and biomedical studies have demonstrated that saikosaponins (SSs), a serious of pentacyclic triterpenoid oleanolic derivatives, are major bioactive ingredients in RB. Saikosaponin A (SSa) and saikosaponin D (SSd) are the most abundant SSs, possessing anti-inflammatory, anti-oxidation, immunoregulation, anti-viral, anti-cancer, and hepatoprotective effects[18]. However, a gap in our knowledge exists regarding the potential effects and mechanisms of SSs on NAFLD. In our recent study of SSs-related acute hepatotoxicity, we employed Multiplexed Isobaric Tagging Technology for Relative Quantitation (iTRAQ)-based proteomic approaches and demonstrated that, without inducing significant liver injury, a single administration of SSs rapidly and persistently regulated the protein expression profile of lipid transportation and metabolism-related genes, such as

Apoa4, *Fabp3*, *Acox1*, *Lipa*, and *Acadl*[19]. These insightful results in combination with the traditional use of RB in the treatment of NAFLD encourage us to further investigate the potential therapeutic effects of SSa and SSd on diet-induced NAFLD and its underlying molecular mechanisms.

In the current study, we evaluate and compare the protective effects of SSa and SSd on hepatic lipid accumulation in high-fat diet (HFD) and glucose-fructose water (HFSW)-induced NAFLD mouse model. The integrative lipidomic and transcriptomic analysis revealed that both SSa and SSd improved disrupted homeostasis of lipid metabolism, yet plausibly through different mechanisms, which was further confirmed *in vitro* in mouse primary hepatocytes. Our data provide experimental evidence supporting that SSs and derivatives may serve as novel therapeutic strategies for the management of NAFLD and associated manifestations.

2. Materials and methods

2.1. Animal study

Male C57BL/6J mice (8-week-old) were purchased from Vital River Laboratory Animal Technology (Beijing, China). Mice were acclimatized under 12 h/12 h light and dark cycle at a constant temperature (22 ± 2 °C) and were provided with standard chow and water *ad libitum*. All animal experiments were approved by the Shandong University Institutional Animal Care and Use Committee (Ji'nan, China). Mice were randomly divided into eight groups: (I) control group (chow diet); (II) fatty liver group [HFSW, Western diet-42% kcal from fat and 0.2% cholesterol (TD.88137, Harlan Laboratories, Inc., Indianapolis, IN, USA), along with a high-fructose-glucose solution (D-glucose: 18.9 g/L and D-fructose: 23.1 g/L) in drinking water][20]; (III−V) HFSW with SSa administration groups; (VI−VIII) HFSW with SSd administration groups. Groups (II−VIII) were all fed with HFSW for 8 weeks. After fed with HFSW for 4 weeks, groups (III−VIII) were intragastrically administered with different doses of SSa (5, 10, and 20 mg/kg) and SSd (5, 10, and 20 mg/kg) once daily for another 4 weeks. Bodyweight, food consumption, and water intake were recorded every other day. At the end of experiment, all mice were sacrificed. Serum was collected and livers were prepared for paraffin sections or frozen in liquid nitrogen.

2.2. RNA-sequencing analysis

Total RNA was extracted from mouse liver tissues. RNA purity was detected by the NanoRhatometer@spectrophotometer (IMPLEN, Santa Clara, CA, USA) and RNA integrity was assessed using the RNA Nano 6000 Assay Kit of the Bioanalyzer 2100 system (Agilent Technologies, Santa Clara, CA, USA). mRNA was purified from total RNA by poly-T oligo-attached magnetic beads (New England Biolabs, Ipswich, MA, USA). Fragmentation was performed using divalent cations under elevated temperature in NEB fragmentation buffer (New England Biolabs). Sequentially, first-strand cDNA and second strand cDNA were synthesized. After purified with AMPure XP system (Beckman Coulter, Beverly, MA, USA), cDNA fragments of 250−300 bp were preferentially enriched. Sequencing library preparation was carried out using NEBNext UltraTM RNA Library Prep Kit for Illumina (NEB) following manufacturer's recommendations and was further sequenced on an Illumina Novaseq platform (Illumina, San Diego, CA, USA) and 150 bp paired-end reads were established. Gene Ontology (GO) and Kyoto Encyclopedia of Genes and Genomes (KEGG) enrichment analysis of differentially expressed genes were performed by the cluster profile R package. Based on GO and KEGG dataset, differentially expressed genes were further analyzed by Gene set enrichment analysis (GSEA). CHIP-X Enrichment Analysis Version 3 (ChEA3) was applied for the transcription factor enrichment analysis, and scores were obtained from TopRank and MeanRank[21].

2.3. Lipidomic analysis

About 250 mg of frozen liver samples (8 biological replicates for each group) were accurately weighed and then pulverized in a Freezer Mixer (Thermo Fisher, Carlsbad, CA, USA) at liquid nitrogen temperature. The samples were extracted in a solvent mixture [MTBE: methanol: water (10:3:2.5, *v*/*v*/*v*)]. The organic phase was collected after incubating at room temperature for 10 min and centrifuging at 1000 × *g* for 10 min. The lower phase was re-extracted with 1 mL of the solvent mixture. The organic phase collected twice was concentrated using a nitrogen blowing device (Thermo Fisher) and reconstituted with 100 μL of isopropanol. Then each sample was analyzed by liquid chromatography/mass spectrometry (LC/MS)/MS instrument (Thermo Fisher). Briefly, samples were injected onto a Thermo Accucore C30 column (150 mm × 2.1 mm, 2.6 μm) (Thermo Fisher) using a 20-min linear gradient at a flow rate of 0.35 mL/min. The column temperature was set at 40 °C. Solvent A was acetonitrile/water (6/4) with 10 mmol/L ammonium acetate and 0.1% formic acid. Solvent B was acetonitrile/isopropanol (1/9) with 10 mmol/L ammonium acetate and 0.1% formic acid. The gradient was generated with solvents A and B as follows: 70% A and 30% B, initial; 70% A and 30% B, 2 min; 57% A and 43% B, 5 min; 45% A and 55% B, 5.1 min; 30% A and 70% B, 11 min; 1% A and 99% B, 16 min; 70% A and 30% B, 18.1 min. Mass spectrometry analysis was performed first in both positive/negative ion switching method in Full MS scan mode. The raw data files generated were processed using the Compound Discoverer 3.01 (CD3.1, Thermo Fisher), including peak alignment, peak picking, and quantitation for each metabolite. Statistical analysis was performed using the statistical software R (version R-3.4.3, University of Auckland, New Zealand, CA, USA), Python (2.7.6 version, Google, Amsterdam, Holland), and CentOS (CentOS release 6.6, Red Hat, Raleigh, NC, USA).

2.4. Isolation and culture of mouse primary hepatocytes

Mouse primary hepatocytes (MPH) were freshly isolated using a two-step collagenase digestion method as previously described[22]. MPH were cultured in William's E medium supplemented with 100 U/mL penicillin, 100 μg/mL streptomycin, 0.1 μmol/L dexamethasone, and 0.1 μmol/L thyroxine (Sigma−Aldrich, St. Louis, MO, USA). All cells were cultured in a humidified cell culture incubator (Thermo Fisher) at 37 °C with 5% CO_2.

2.5. Statistical analysis

Results are representative of at least three independent experiments or at least eight mice for each group. Data were expressed as mean ± standard error of mean (SEM) and statistical analysis was performed using Prism 7.0 (GraphPad, La Jolla, CA, USA). Multiple comparisons were performed by one-way ANOVA with

Tukey's *post-hoc* test. $P < 0.05$ was considered statistically significant (see the Supporting Information for detailed descriptions of other experimental materials and methods).

3. Results

3.1. SSa and SSd ameliorated HFSW-induced hepatic steatosis in mice

To reveal the potential protective effects and detailed mechanisms of SSa and SSd on fatty liver, mice were fed an HFSW diet for 8 weeks and were co-administered with SSa or SSd from Week 5 as described in the Materials and methods. The body weight and the intake of food and water were recorded twice a week. As shown in Fig. 1A, both SSa and SSd inhibited HFSW-induced weight gain, especially for medium and high doses of SSa, without affecting the food and water intake of mice (Supporting Information Fig. S1). Serum biochemistry assays then demonstrated that HFSW significantly induced liver injuries, as indicated by elevated alanine transaminase (ALT) and aspartate transaminase (AST) levels, which were all markedly protected by the administration of SSa and SSd (Fig. 1B). As expected, HFSW also significantly increased the lipid accumulation in the serum, including triglycerides (TG) and cholesterol in both LDL and

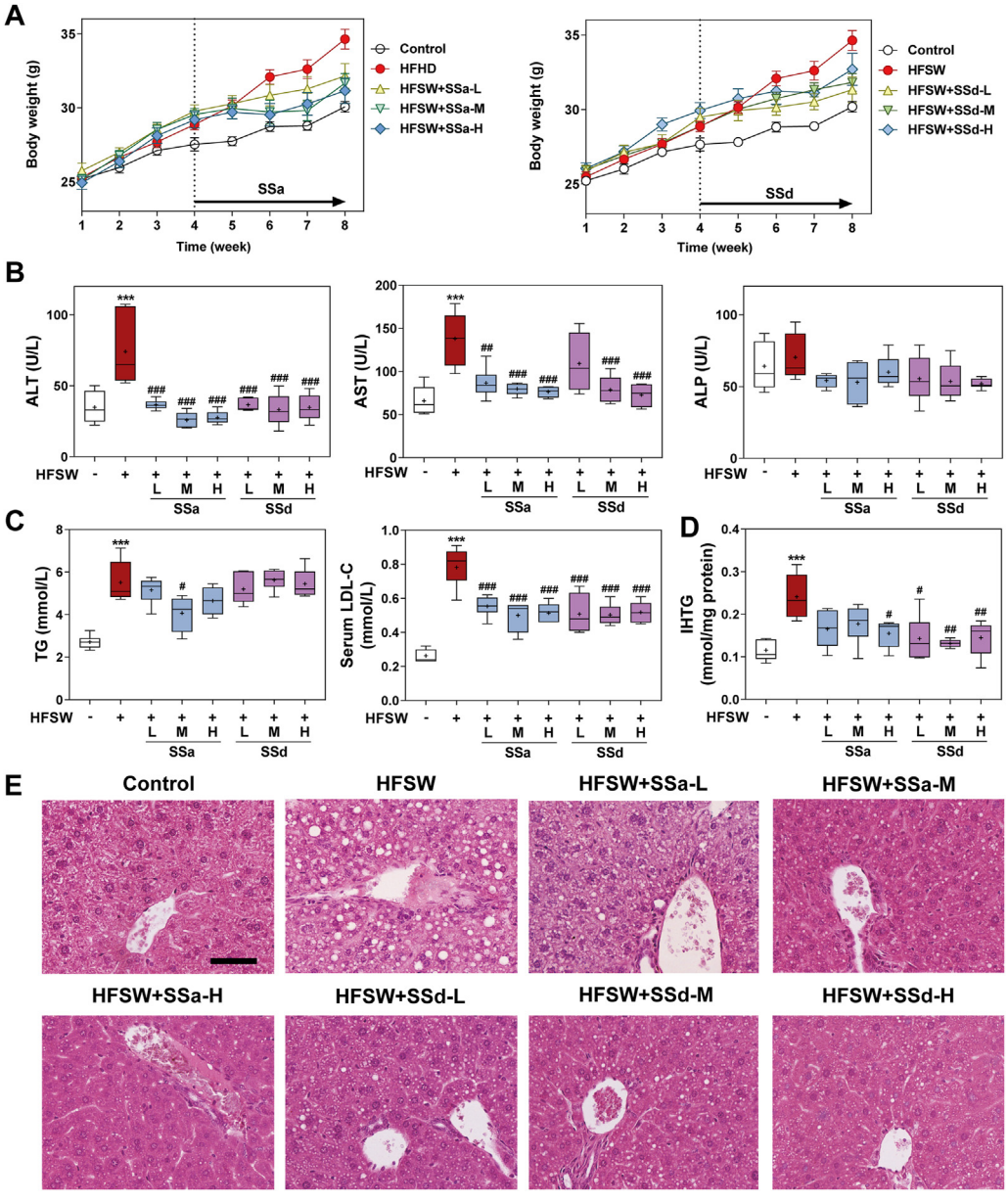

Figure 1 SSa and SSd ameliorated HFSW-induced hepatic steatosis and liver injury. Mice were fed chow diet or HFSW diet for 8 weeks, and administered with either SSa or SSd as described in the Material and methods. (A) Body weights of mice in different groups. (B) The serum ALT, AST, and ALP activity levels. (C) The serum triglycerides (TG) levels and low-density lipoprotein-cholesterol (LDL-C) levels. (D) The intrahepatic TG (IHTG) levels. (E) Representative images of hematoxylin and eosin staining of liver paraffin sections. Scale bar: 50 μm. Results are presented as mean ± SEM ($n \geq 8$ mice in each group). $^{***}P < 0.001$ *vs.* control group; $^{\#}P < 0.05$, $^{\#\#}P < 0.01$, $^{\#\#\#}P < 0.001$ *vs.* HFSW group.

high-density lipoprotein (HDL). Interestingly, SSa significantly reduced both serum TG and LDL-cholesterol levels but SSd only significantly decreased LDL-cholesterol levels in the serum (Fig. 1C). The effect of both SSa and SSd on HDL-cholesterol was minimal (data not shown). We further determined the TG accumulation in the liver. As shown in Fig. 1D, the intrahepatic TG levels were significantly increased by 2.5-fold in the HFSW group, which were significantly reversed by both SSa and SSd treatment. In line with this finding, liver histopathology study indicated that SSa and SSd significantly and dose-dependently inhibited the HFSW-caused lipid accumulation and extensive steatosis as indicated by reduced number and size of lipid droplets in hepatocytes (Fig. 1E).

3.2. *SSa and SSd extensively modulated hepatic lipid profile*

To further verify the effects of SSa and SSd on lipid metabolism in the fatty liver, a lipidomic analysis was performed to determine the intrahepatic lipid profile transformation in HFSW, SSa-medium (SSa-M), and SSd-M groups *vs*. the control group. Principal component analysis (PCA) analysis and volcano plots of differentially altered lipid metabolites (DALs) suggested that the intrahepatic lipid profiles were remarkably shifted in HFSW-fed mice, while SSa and SSd treatment further modulated the HFSW-induced dysregulation of lipid metabolism, as observed in both positive and negative detection modes of LC−MS/MS lipidomic analysis (Supporting Information Fig. S2A and S2B). Hierarchical cluster analysis further subdivided all DALs into 6 clusters based on alteration patterns, and 4 clusters of interests were labeled in Fig. 2A. As shown in Fig. 2B, the relative contents of DALs categorized in cluster 1 and cluster 2 were significantly upregulated in SSa and SSd groups when compared to the HFSW group. It is also noteworthy that the levels of DALs in cluster 3 and cluster 4 were all significantly upregulated by HFSW feeding, which were then reversed by SSa and SSd treatments. We then found that 23.79%, 16.72%, and 15.76% of DALs in cluster 1 belongs to the lipid classes of phosphatidylcholine (PC), phosphatidylethanolamine (PE), and sphingolipids, respectively. In cluster 2, 7.09% of DALs are acyl-carnitines (ACARs), 6.3% are acyl-amino acids (acyl-AA), and 6.3% are PC. These DALs were only moderately upregulated by SSa, yet dramatically increased in SSd group, suggesting that these DALs were specific targets of SSd but not SSa. The lipidomic analysis also showed that 24.64% of DALs in cluster 3 were diacylglycerol (DAG), and 18.84% were TG. Additionally, when compared to SSa, SSd was more efficient in regulating the contents of DALs in cluster 4, in which 10.75% were sphingolipids, 9.68% were PC, and 6.45% were phosphatidic acids (PHA). To further determine the preferences of SSa and SSd on regulating lipid metabolism in fatty liver, we plotted the fold changes (SSa *vs*. HFSW and SSd *vs*. HFSW) of DALs belonging to 15 lipid classes. Both SSa and SSd significantly upregulated the contents of PE and acyl-AA, and significantly reduced the accumulation of PHA and DAG with similar potency. On the other hand, as shown in Fig. 2D and Supporting Information Fig. S3A, SSa modulated the TG profiles on a large scale, both positively and negatively. However, the effects of SSd on TG metabolism were not significant. More interestingly, SSd significantly shifted the profile of ACARs in the fatty liver, suggesting the potential implication of SSd in lipid catabolism, given the essential role of ACARs formation in the initiation of fatty acid β-oxidation (Fig. 2E and Supporting Information Fig. S3B). These findings suggested that although both SSa and SSd ameliorated HFSW-induced hepatic steatosis, the underlying mechanisms were varied since the preferences of SSa and SSd on modulating lipid profiles were different.

3.3. *SSa and SSd extensively regulated the expression of genes involved in lipid metabolism*

Transcriptomic analysis using RNA-sequencing (RNA-seq) was performed to reveal the underlying mechanisms and potential molecular targets of SSa and SSd in regulating lipid metabolism. As shown in Supporting Information Fig. S4A and S4B, a total of 2528 genes were identified as differentially expressed genes (DEGs, $P < 0.05$) in the HFSW group when compared to the control group, with 1208 upregulated and 1320 downregulated. These DEGs were significantly enriched in lipid metabolism, according to GO-biological process (GO: BP) analysis (Supporting Information Fig. S4C). RNA-seq results further demonstrated that all doses of SSa and SSd significantly shifted the transcriptomic profile in the livers of HFSW-fed mice (Fig. 3A and Supporting Information Fig. S5A and S5B). GSEA analysis suggested that the phenotype of NAFLD (KEGG entry: MMU04932) was potentially enriched in the HFSW group and was reversed by almost all SSs treatment groups, except for SSa at a low dose, which was consistent with our findings in the histopathological and lipidomic analysis (Fig. 3B). As shown in Fig. 3C, GO analysis suggested that DEGs in SSa-M *vs*. HFSW and SSa-high (SSa-H) *vs*. HFSW were significantly enriched in several GO: BP terms related to lipid metabolism, such as neutral lipid metabolic process, glycerol lipid metabolic process, and regulation of lipid metabolic process. On the other hand, SSd-related DEGs were enriched in triglyceride metabolic process in both medium-dose group and high-dose group, and DEGs in SSd-H *vs*. HFSW were also enriched in acylglycerol metabolic process and lipid homeostasis (Fig. 3D). These findings suggested that both SSa and SSd modulated intrahepatic lipid profiles by extensively regulating the expression of genes involved in lipid metabolism.

3.4. *SSa and SSd regulated glycerol lipid metabolism in fatty liver*

The expression profile of DEGs enriched in the GO term of glycerolipid metabolism was shown as a heatmap in Fig. 4A. GSEA analysis also suggested that the upregulation of genes involved in glycerolipid metabolism (KEGG entry: MMU00561) were enriched in SSa and SSd groups, especially at higher doses, suggesting the regulative effects of SSs on glycerolipid metabolism (Fig. 4B). These DEGs were further categorized into two subsets depending on their molecular functions. Interestingly, we found that 9 out of 14 DEGs promoting glycerol lipid biosynthesis and storage, including *Cidea*, *Lpin1*, *Pnpla3*, *Mogat1*, and *Fitm1*[23], were downregulated by medium and high doses of SSa and all doses of SSd (Fig. 4A, upper panel). As shown in the lower panel of Fig. 4A, critical genes responsible for glycerol lipid activation and catabolism, including *Gk*, *Ces1d*, *Lipg*, and *Lipe* were all significantly upregulated by SSa and SSd[23]. Real-time PCR further verified the findings of RNA-seq analysis, and further confirmed that SSd was more efficient in inducing the expression of genes implicated in glycerol lipid degradation, as indicated by the mRNA levels of *Ces1d* and *Lipg* (Fig. 4C and D). As shown in Fig. 4E and Supporting Information Fig. S6A, the lipidomic analysis revealed that DAG

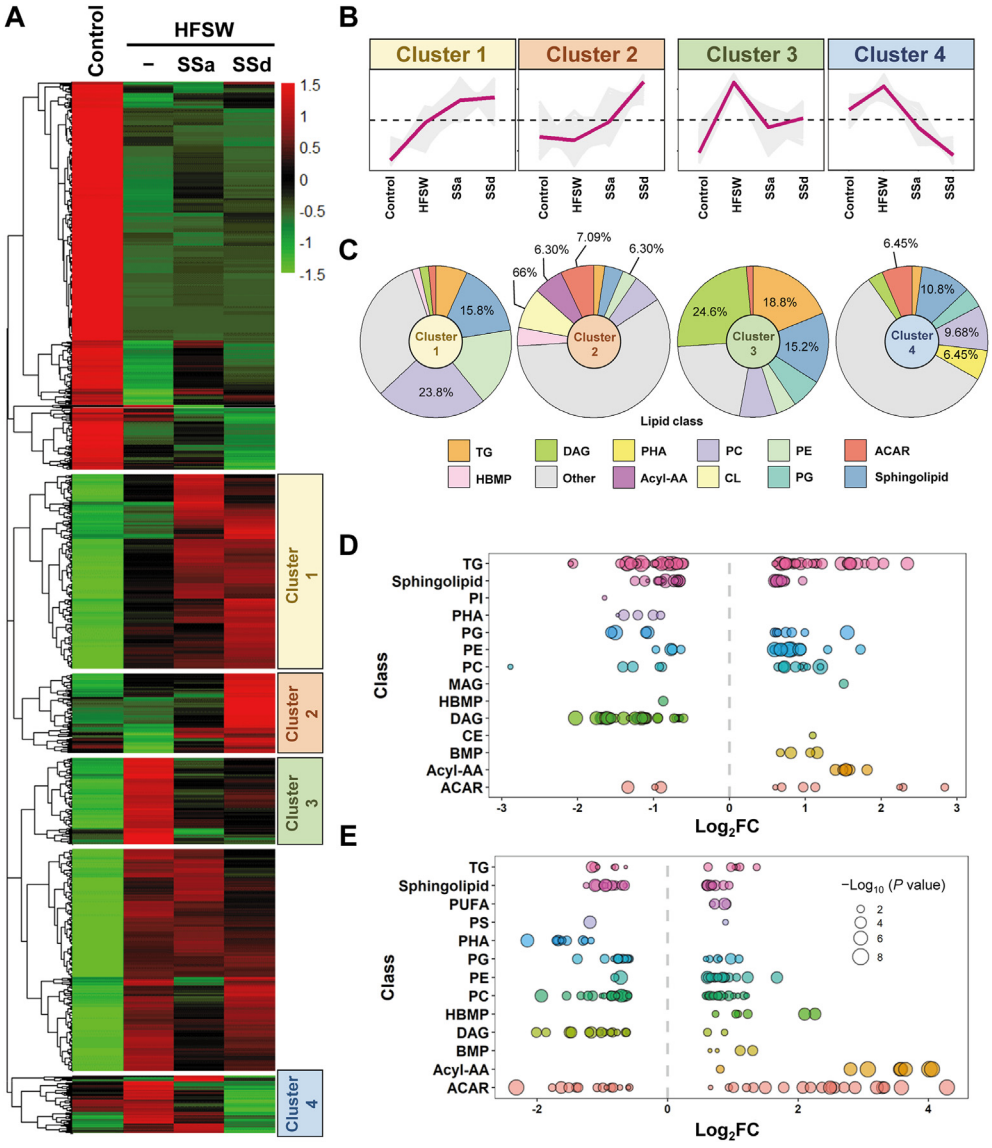

Figure 2 SSa and SSd extensively modulated hepatic lipid metabolism. Lipidomic analysis was performed on mice liver tissue samples (n = 8). (A) Significant differentially altered lipids (DALs) were clustered and plotted as a heatmap. (B) Four clusters (clusters 1−4) were highlighted, and the trend lines indicating the change of intrahepatic levels of these DALs were shown. (C) DALs in each cluster were subcategorized based on their lipid classes. (D) and (E) Fold changes of DALs belonging to different lipid classes upon SSa and SSd challenges (SSa *vs.* HFSW and SSd *vs.* HFSW) were plotted in panels (D) and (E), respectively. The size of each dot represents $-\log_{10}$ (P value).

levels were significantly increased in HFSW-induced fatty liver, and both SSa and SSd significantly reversed intrahepatic DAG accumulation. Integrative analysis of transcriptomic and lipidomic data strongly suggested that the clearance of DAGs by SSa and SSd were attributed to the increased expression of TG and DAG hydrolyzing enzymes and decreased expression of DAG producing enzyme Lpin1. Furthermore, SSa and SSd significantly decreased the PHA contents in the fatty liver by 1.5−3-fold and thus contributed to the reduction of DAG levels, since PHA was also an important substrate for DAG synthesis (Fig. 4E and F, and Supporting Information Fig. S6B). These findings were also in accordance with SSa- and SSd-induced downregulation of *Pnpla3*, the enzyme catalyzing PHA production.

3.5. SSa and SSd hampered fatty acid biosynthesis and promoted fatty acid degradation

A disrupted balance between fatty acid biosynthesis and degradation is the major cause of lipid metabolism dysregulation and lipotoxicity in the pathogenesis of fatty liver diseases. Although fatty acid biogenesis was not the top ten enriched terms in the GO analysis, DEGs related to this process were plotted in Fig. 5A as a heatmap. Essential genes involved in *de novo* fatty acid biosynthesis, including *Acaca* and *Fasn*, were all significantly downregulated by SSa and SSd. On the other hand, several genes implicated in the elongation and desaturation of fatty acids, such as *Fads2*, *Fads3*, *Fads6*, and *Elovl6*, were upregulated by SSd but not SSa. Both real-time PCR and Western blot analysis

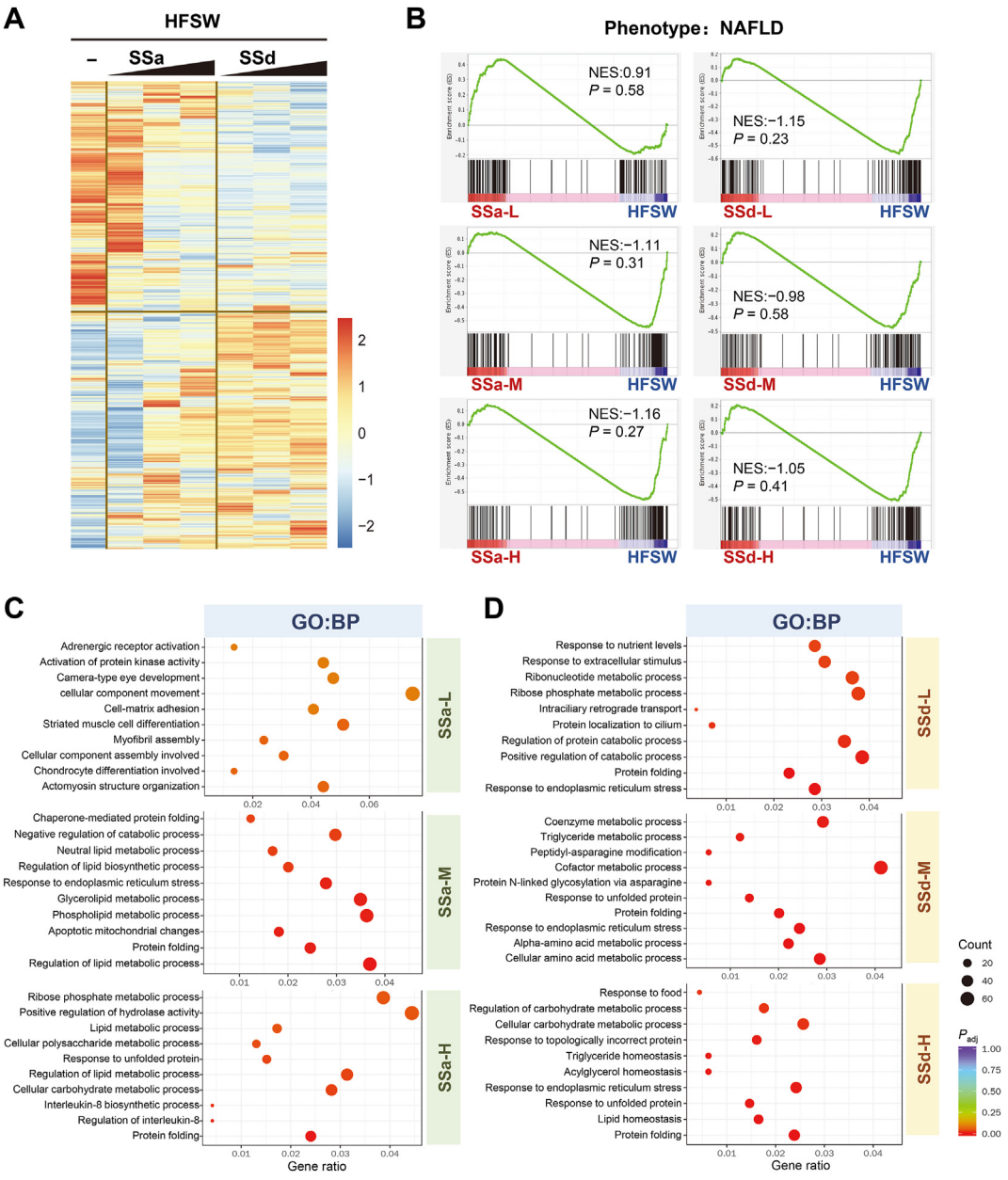

Figure 3 SSa and SSd regulated hepatic transcriptome in a large scale. RNA-seq analysis was performed on mice liver tissue samples ($n = 4$). (A) Heatmap represented the expression profile of differentially expressed genes (DEGs) ($P < 0.05$) identified in the comparison of SSa treatment groups (SSa-L, SSa-M, and SSa-H) *vs.* HFSW group, and SSd (SSd-L, SSd-M, and SSd-H) treatment groups *vs.* HFSW group. (B) Gene set enrichment analysis (GSEA) plot for KEGG entry: NAFLD based on DEGs in SSa and SSd groups *vs.* HFSW group. NES, normalized enrichment score. (C) and (D) GO pathway enrichment analysis (BP: biological process) based on DEGs in SSa and SSd groups *vs.* HFSW group. P_{adj}, adjusted *P* value.

demonstrated that HFSW slightly induced the expression of ACCα and FASN, which were then significantly downregulated by SSa and SSd (Fig. 5B and C). Sterol regulatory element-binding protein 1 (SREBP-1) has been well-characterized as the master regulator of fatty acid biogenesis and sterol metabolism by transcriptionally modulating gene expression, including *Acaca* and *Fasn*[24]. As shown in Fig. 5D, the mRNA level of *Srebf1* (gene encoding SREBP-1) was slightly increased in HFSW-fed mice and was not significantly changed after SSa and SSd treatment, except for SSa-M group. Since the maturation of SREBP-1, depending on sterol regulatory element-binding protein cleavage-activating protein 1 (SCAP1)-mediated cleavage on the ER, is essential for its function as a transcription factor, we determined the protein levels of cleaved SREBP-1 by Western blot to indicate its cytosolic activation[25]. Interestingly, SSa and SSd did not affect the protein levels of uncleaved SREBP-1 (125 kD), yet inhibited its maturation, as indicated by the decreased protein levels of mature SREBP-1 (60 kD) (Fig. 5E). However, according to RNA-seq data, only part of SREBP-1 downstream genes was downregulated by SSa and SSd, the others were paradoxically upregulated (Fig. 5F). These results suggest that SSa and SSd modulated fatty acid biosynthesis in a complicated way.

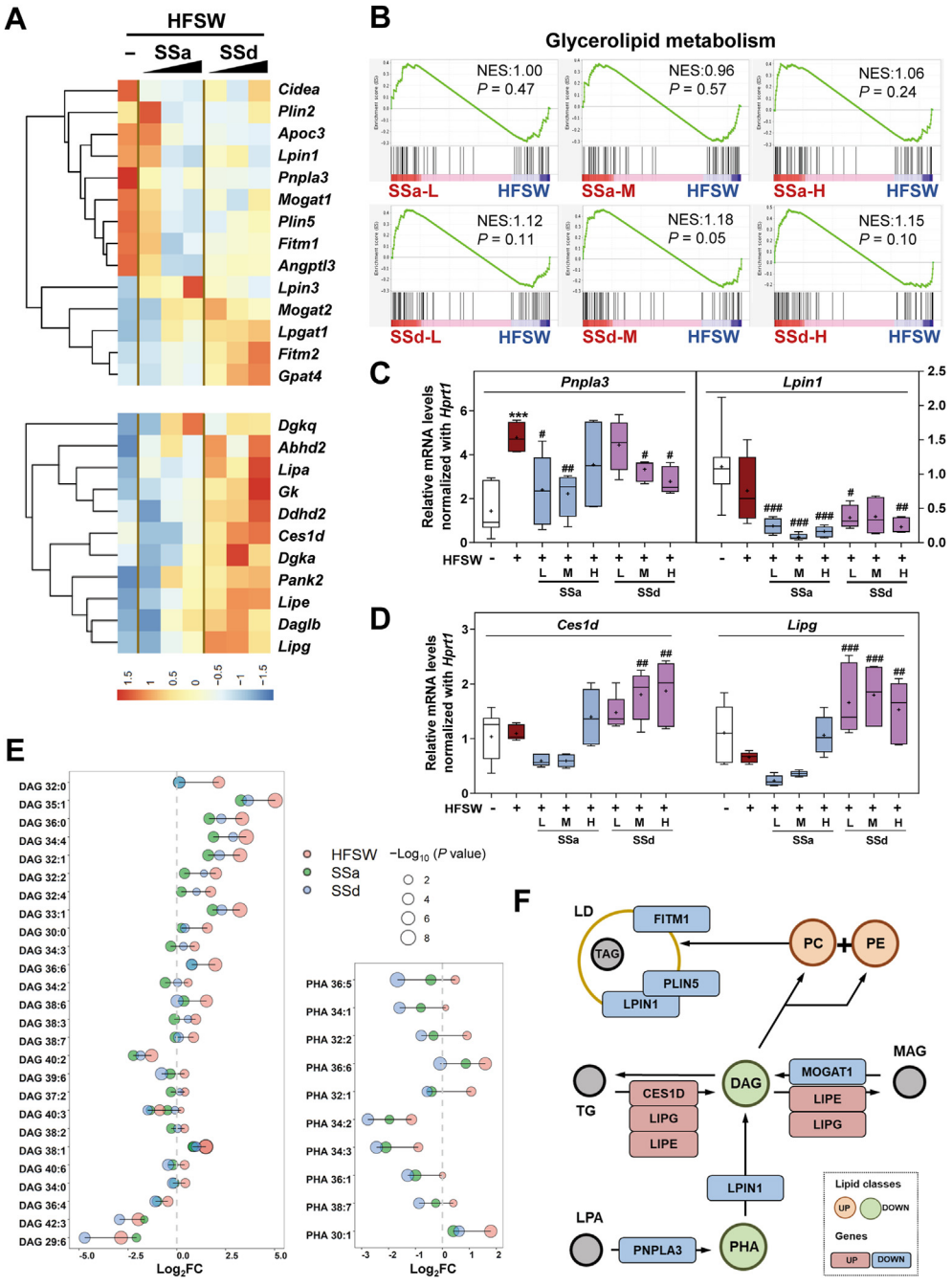

Figure 4 Effects of SSa and SSd on glycerollipid metabolism. (A) The expression profile of DEGs implicated in the metabolism of glycerolipid was shown as heatmap. (B) GSEA plot for KEGG entry: glycerollipid metabolism based on DEGs. (C) and (D) The relative mRNA levels of *Pnpla3* and *Lpin1* (C) and *Ces1d* and *Lipg* (D) were determined by real-time PCR and normalized using *Hprt1* as an internal control. Results are presented as mean ± SEM ($n \geq 6$ mice in each group). $^{***}P < 0.001$ *vs.* control group; $^{\#}P < 0.05$, $^{\#\#}P < 0.01$, $^{\#\#\#}P < 0.001$ *vs.* HFSW group. (E) The changes of intrahepatic levels of diacylglycerols (DAG) and phosphatidic acids (PHA) in the treatment group (SSa and SSd) and model group (HFSW), when compared to the control group. (F) The biological process of glycerolipid metabolism. The orange and green dots represented increased and decreased lipids after SSa and SSd treatment, respectively. The red and blue squares represented upregulated and downregulated genes upon SSa and SSd challenges, respectively.

We further investigated the regulative effects of SSa and SSd on fatty acid degradation. As shown in Fig. 6A, a total of 18 genes involved in fatty acid catabolism were identified, and 13 of these genes were moderately upregulated by SSa and remarkably induced by SSd. *Acsl1*, *Acsm3*, and *Acsm5*, which were key enzymes catalyzing the transformation of fatty acid into their active form fatty acyl-CoA, *Acox1* and *Acox3*, which were responsible for the degradation of VLCFA in the peroxisome, and *Cpt1a*, *Acad10*, *Acad12*, and *Slc27a1*, which were critical for fatty acid transportation and β-oxidation, were all included in this gene set. GSEA analysis further demonstrated that upregulated genes involved in fatty acid degradation (KEGG entry: MMU00071) were enriched in

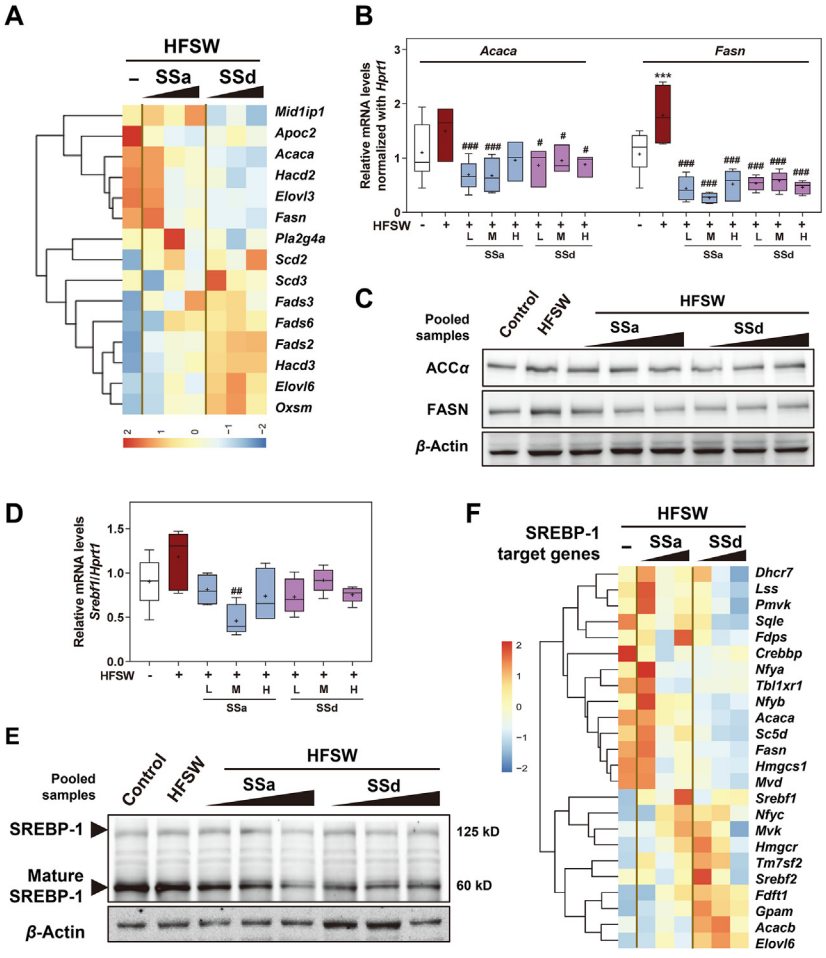

Figure 5 Effects of SSa and SSd on the regulation of fatty acid biogenesis. (A) The expression profile of DEGs implicated in the biosynthesis of fatty acid was shown as heatmap. (B) The relative mRNA levels of *Acaca* and *Fasn* were determined by real-time PCR and normalized using *Hprt1* as an internal control. (C) The relative protein levels of ACCα and FASN were determined by Western blot analysis and using β-actin as a loading control. Representative images of immunoblots were shown ($n = 6$ mice, pooled samples). (D) The relative mRNA level of *Srebf1* was determined by real-time PCR and normalized using *Hprt1*. (E) Representative immunoblot images of SREBP-1 and mature SREBP-1 were shown and β-actin was used as a loading control ($n = 6$ mice, pooled samples). (F) The expression profile of SREBP-1 target genes was presented as heatmap. Results were presented as mean ± SEM ($n \geq 6$ mice in each group). $^{***}P < 0.001$ *vs.* control group; $^{\#}P < 0.05$, $^{\#\#}P < 0.01$, $^{\#\#\#}P < 0.001$ *vs.* HFSW group.

SSd-M and SSd-H groups, when compared to HFSW group, suggesting that SSd was more potent in promoting fatty acid degradation than SSa (Fig. 6B). Real-time PCR results further confirmed the findings in RNA-Seq analysis, showing that SSd, but not SSa, significantly induced *Cpt1a*, *Acsl1,* and *Acox1* expression in fatty liver in a dose-related manner (Fig. 6C). CPT-1α (encoded by *Cpt1a* gene), catalyzing the transfer of the fatty acid-CoA onto carnitine, is essential for the uptake of fatty acid by mitochondria and is the rate-limiting enzyme of FA β-oxidation. In addition to its mRNA levels, the protein levels of CPT-1α were also increased after SSd treatment (Fig. 6D). Along with these findings, the intrahepatic levels of ACARs, the catalytic products of CPT-1α, were dramatically modulated by SSs. Interestingly, the levels of all medium-chain ACARs and 12 out of 15 long-chain ACARs were increased in both SSa and SSd groups. However, the levels of 6 out of 8 very-long-chain ACARs were decreased in the SSd group, when compared to HFSW groups. These results were probably attributed to SSd-mediated induction of ACOXs expression and thus activation of peroxisomal degradation of VLCFA, which drained out the precursor of very-long-chain ACARs (Fig. 6E and F).

We further confirmed the protective effects of SSa and SSd on hepatic steatosis *in vitro* in MPH. As shown in Fig. 7A, oleic acid (OA) and palmitic acid (PA) in a combination of 500 and 250 μmol/L (OA:PA) resulted in significant TG accumulation and lipid droplet formation in 24 h, both SSa (0.3−1.2 μmol/L) and SSd (0.08−0.3 μmol/L) ameliorated the steatosis phenotype induced by OA:PA, as indicated by oil red O staining, and was supported by intracellular TG assay (Fig. 7B). For FA biosynthesis genes, SSa and SSd significantly decreased the expression of *Acaca* but not *Fasn* under normal conditions. OA:PA significantly downregulated the expression of both *Acaca* and *Fasn*, which were significantly suppressed by SSa and SSd (Fig. 7C). For FA degradation genes, as expected, SSa and SSd dose-dependently upregulated the expression of *Ppara*, *Acox1*, and *Cpt1a*, even with the presence of OA:PA (Fig. 7D). These results strongly demonstrated that SSa and SSd, even at concentrations lower than

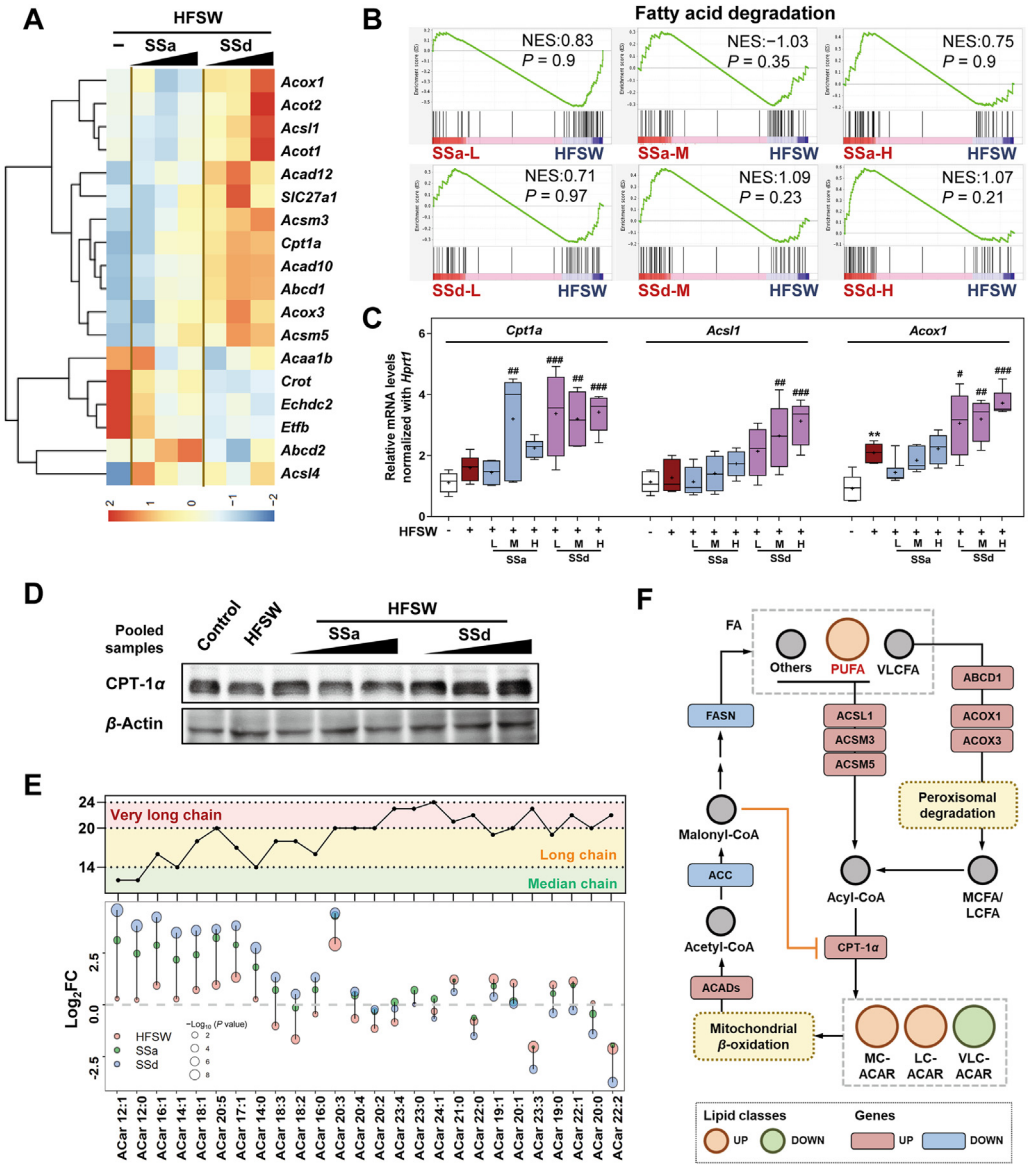

Figure 6 The effect of SSa and SSd on fatty acid degradation. (A) The expression profile of DEGs implicated in the fatty acid catabolism was shown as heatmap. (B) GSEA plot for KEGG entry: fatty acid degradation based on DEGs. (C) The relative mRNA levels of *Cpt1a*, *Acsl1*, and *Acox1* were determined by real-time PCR and normalized with *Hprt1*. (D) The protein level of CPT-1α was determined by Western blot analysis using β-actin as a loading control. Representative immunoblot images were shown ($n = 6$ mice, pooled samples). (E) The changes of intrahepatic levels of acyl-carnitines (ACARs) in the treatment group (SSa and SSd) and model group (HFSW), when compared to the control group. (F) The biological process of fatty acid biosynthesis and degradation. The orange and green dots represented increased and decreased lipids after SSa and SSd treatment, respectively. The red and blue squares represented upregulated and downregulated genes upon SSa and SSd challenges, respectively. Results were presented as mean ± SEM ($n \geq 6$ mice in each group). $^{**}P < 0.01$ *vs.* control group; $^{\#}P < 0.05$, $^{\#\#}P < 0.01$, $^{\#\#\#}P < 0.001$ *vs.* HFSW group.

1 μmol/L *in vitro*, were promising therapeutic candidates against fatty liver diseases by promoting fatty acid metabolism.

3.6. SSa and SSd regulated lipid metabolism genes expression via transcription factors

The above findings demonstrated that SSa and SSd modulated the expression profile of lipid metabolism-related genes on a large scale, suggesting that upstream transcription factors (TF), instead of single lipid catalytic enzyme, maybe the primary molecular targets of SSs. Thus, based on a gene list of upregulated DEGs (SSa *vs.* HFSW and SSd *vs.* HFSW) enriched in GO term of lipid metabolism, Chip-X Enrichment Analysis Version 3 (ChEA3) analysis were performed to predict the involved TFs. As shown in Fig. 8A, according to the two embedded scoring systems in ChEA3, the top ten TFs with more than 10 target genes overlapped with DEGs were highlighted. The expression patterns of these TFs upon SSa and SSd challenges were further shown in Fig. 8B. Interestingly, the expression of *Cebpa* and *Mlxipl* were suppressed by SSd when compared to HFSW group, whereas

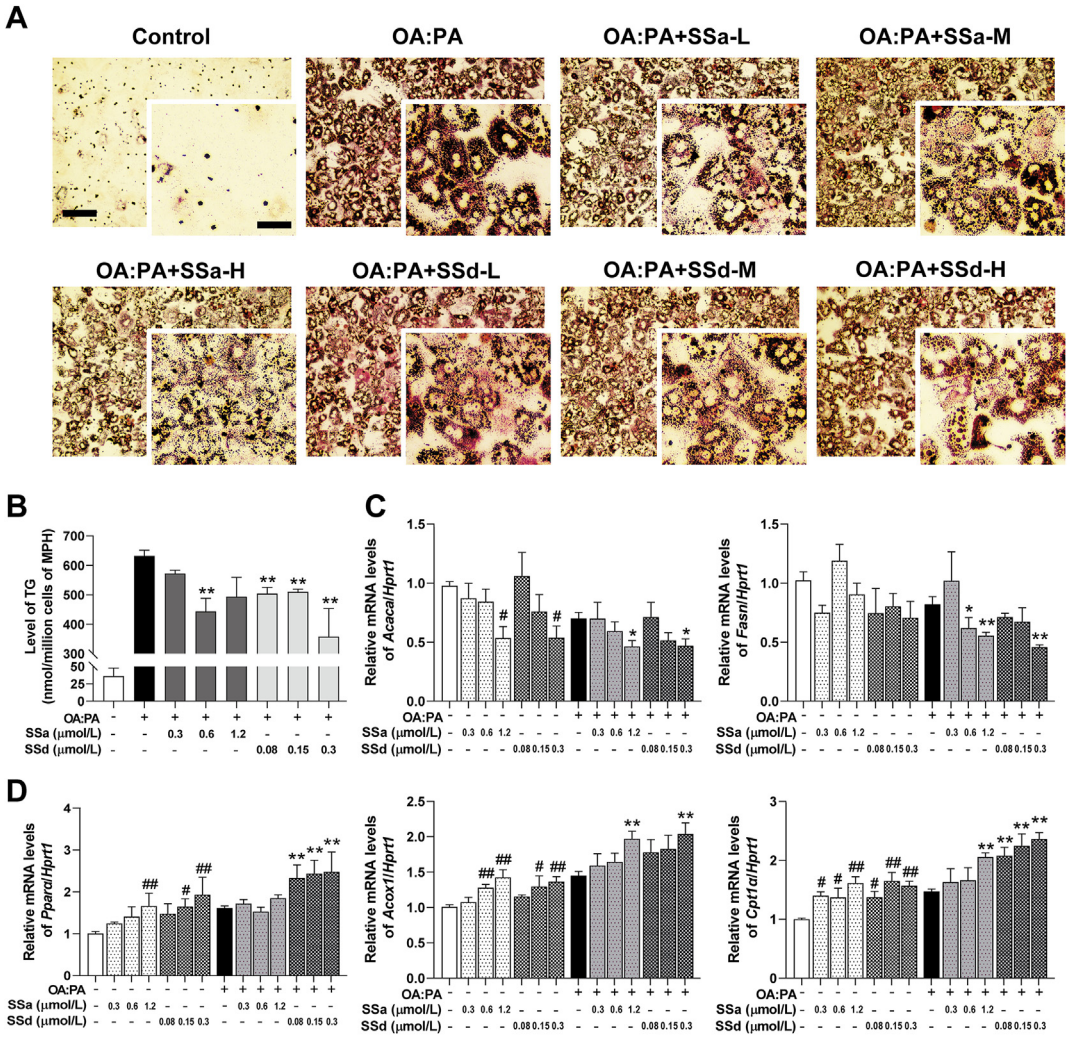

Figure 7 The effect of SSa and SSd on fatty acid metabolism in primary liver cells. Mouse primary hepatocytes (MPH) were incubated with OA:PA (500 μmol/L:250 μmol/L) and treated with SSa and SSd as indicated for 24 h. (A) Representative images (scale bar: 100 μm) of oil red O staining of MPH and magnified images (scale bar: 50 μm). (B) The intracellular TG levels were determined as described in the method. (C) and (D) The relative mRNA levels of *Acaca* and *Fasn* (C), and *Ppara*, *Acox1*, and *Cpt1a* (D) were determined by real-time PCR and normalized using *Hprt1* as an internal control. Results were presented as mean ± SEM ($n = 3$). $^{\#}P < 0.05$, $^{\#\#}P < 0.01$ *vs.* control group; $^{*}P < 0.05$, $^{**}P < 0.01$ *vs.* OA:PA group.

Ppara (encoding PPARα), *Pparg* (encoding PPARγ), *Nr1h3* [encoding liver X receptor alpha (LXRα)], *Esrra* [encoding estrogen-related receptor alpha (ERRα)], *Nr1i3* [encoding constitutive androstane receptor (CAR)], and *Srebf1* were upregulated by both SSa and SSd. The molecular simulation was then employed to further explore the potential binding of SSa, SSd, and their *in vivo* metabolites with these upregulated TFs (Fig. 8C)[18]. In Fig. 8D, the color of each dot represented the binding free energy (BFE) of compounds, and the size of dots indicated the similarity of the binding affinity of SSs and metabolites when compared to the original ligands in the protein crystal structure complex, as calculated following the instruction in the Materials and methods. Generally, SSa, SSd, and their metabolites were not likely ligands for PPARγ, CAR, retinoid X receptor alpha (RXRα), androgen receptor (AR), and ERRα, based on the criteria of binding free energy less than −5.0 kJ/mol. It is noteworthy that SSa was a potential ligand for PPARα (−22.2 kJ/mol) and LXRα (−32.7 kJ/mol), yet with low predicted affinity, and SSd was plausible stronger PPARα ligand than SSa, as indicated by lower binding free energy (−29.3 kJ/mol). The molecular docking results further showed that the binding mode of SSa and SSd with PPARα was similar to that of synthetic PPARα agonist, TIPP703 (Fig. 8E). The binding free energy of SSa metabolites with PPARα, including saikogenin a (SGa, −31 kJ/mol), saikogenin h (SGh, −26.8 kJ/mol), and prosaikogenin f (pSGf, −28.1 kJ/mol), was lower than that of SSa. Similarly, SSd metabolites, such as SGd (−31.8 kJ/mol) and prosaikogenin g (pSGg, −32.2 kJ/mol) were also more potent ligands for both PPARα. These results suggested that *in vivo* metabolism might contribute to the regulative effects of SSa and SSd on gene expression. Since the primary targets of LXRα, mainly lipogenic genes like *Fasn* and *Scd1*, were either downregulated or not changed by SSs treatment, we focused on the potential effects of SSa and SSd on PPARα, the master TF regulating lipid degradation[26]. Interestingly, in line with the

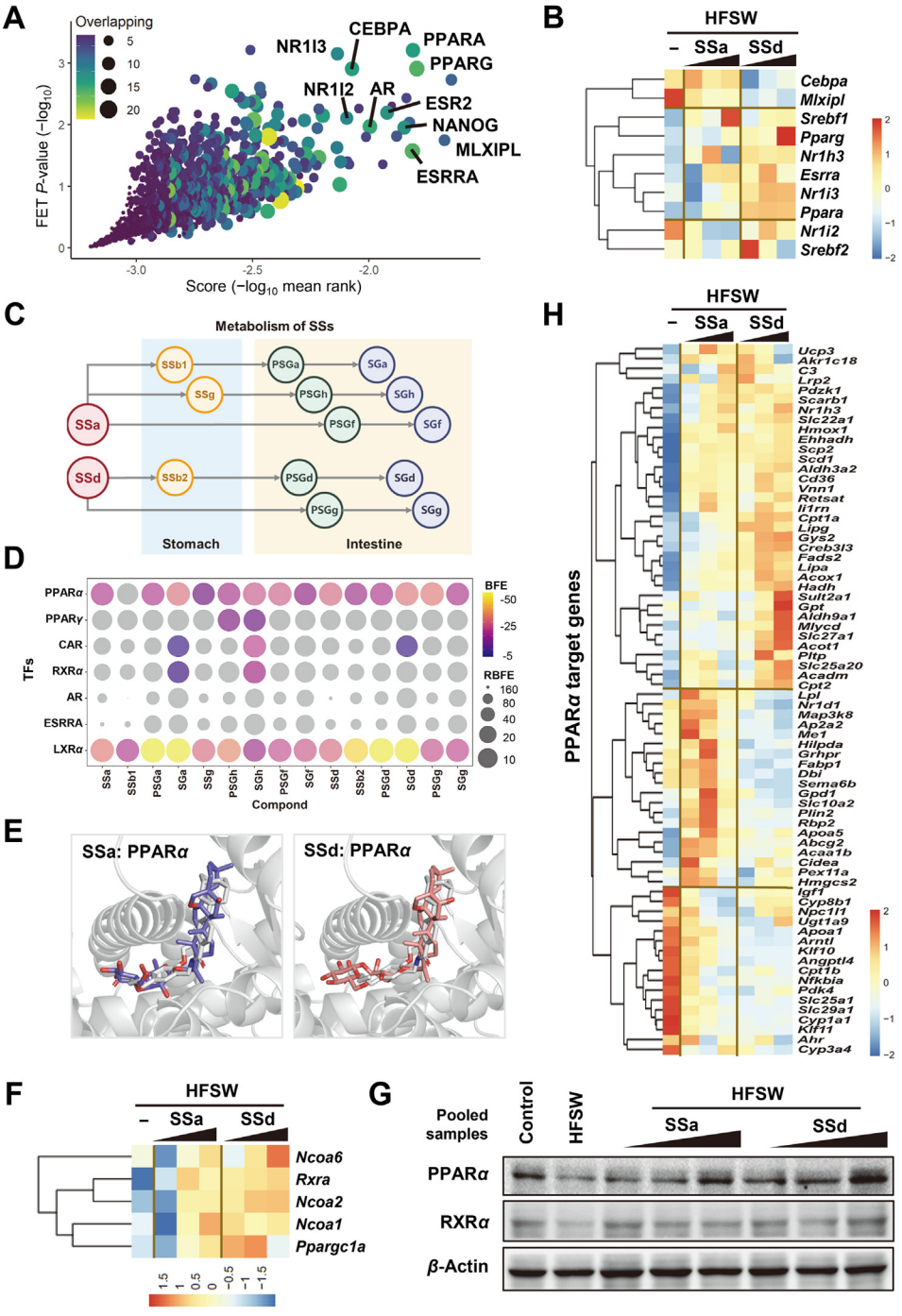

Figure 8 Regulative effects of SSa and SSd on transcription factors (TFs) involved in lipid metabolism. (A) Transcription factors enrichment analysis (TFEA) plot based on the upregulated DEGs enriched in lipid metabolism pathways. (B) The expression profile of predicted TFs involved in the regulation of lipid metabolism. (C) The *in vivo* biotransformation and metabolism of SSa and SSd. (D) Molecular docking results of SSs and metabolites binding to indicated TFs. Binding free energy (BFE) and relative BFE (RBFE) indicating the potential binding affinity were calculated as instructed in the method. (E) The representative images for the binding mode of SSa (purple), SSd (pink), and synthetic PPARα agonist TIPP703 (white) with the crystal structure of PPARα (PDB ID: 2ZNN, grey). (F) The expression profile of PPARα and its coactivators. (G) The protein levels of PPARα and RXRα in the liver were determined by Western blot using β-actin as a loading control (n = 6 mice, pooled samples). (H) The expression profile of PPARα target genes was presented as a clustered heatmap.

induced PPARα expression, RNA-seq analysis suggested that the expression of several co-factors of PPARα, including *Ncoa1*, *Ncoa2*, *Ncoa6*, *Rxrα*, and *Ppargc1a*, were also increased by SSa and SSd (Fig. 8F)[27,28]. Western blot analysis further demonstrated that the protein levels of both PPARα and RXRα were decreased upon HFSW feeding, which were reversed by SSa and SSd in a dose-related manner (Fig. 8G). Furthermore, by investigating the expression patterns of PPARα target genes, we found that more

than half of these target genes were upregulated by both SSa and SSd, about 25% of them were induced by SSa treatment, and only less than 25% were downregulated by SSs (Fig. 8H). These results strongly suggested that SSa, SSd, and specific metabolites regulated hepatic lipid metabolism by activating TFs network, including PPARα, RXRα, and LXRα, although further experimental evidence is still required for validation.

4. Discussion

NAFLD, with continuously increasing morbidity, represents one of the most common risk factors of advanced stages of liver diseases, related metabolic complications, and subsequent death, and has become a substantial burden for the economy and healthcare system. However, numerous attempts to treat NAFLD have failed in the clinical trial, leading to the absence of approved therapeutic options. TCM has been clinically practiced for the treatment of diseases with similar manifestations of NAFLD for thousands of years, and RB is regarded as one of the most frequently used herbal products in these TCM formulas. We previously demonstrated that a single dose of purified SSs fraction, containing SSa, SSb1, SSb2, and SSd, broadly and rapidly regulated the hepatic levels of proteins involved in lipid transportation and metabolism by applying iTRAQ proteomic analysis[19]. In the current study, we established a NAFLD mouse model by a combination of HFD and fructose-glucose drinking water and demonstrated that both SSa and SSd improved NAFLD, as indicated by reduced hepatocyte ballooning area and decreased intrahepatic and serum TG levels and LDL-cholesterol, and protected NAFL-related liver injury, as illustrated by decreased serum AST and ALT levels. Furthermore, by applying integrative lipidomic and transcriptomic analysis, we systemically evaluated the specific effects of SSa and SSd on the hepatic lipid metabolic spectrum and the expression profile of genes implicated in lipid metabolism.

Interestingly, the effects of SSa and SSd on HFSW-induced dysregulation of lipid profile were remarkably different, although SSa and SSd are identical in molecular formula (Figs. 2 and 4). SSa profoundly and bidirectionally altered the accumulation of TG in the liver, namely upregulated more than 20 types of TG with distinct fatty acid chains and significantly downregulated more than 30 types of TG. Meanwhile, SSd only upregulated and downregulated 7 and 6 types of TG, respectively. These findings were associated with the different effects of SSa and SSd on the expression of genes involved in the formation and enlargement of lipid droplets (LDs). LDs are specialized subcellular organelle storing excessive fatty acids as TGs. The biogenesis, deposition, and breakdown of intracellular TG were tightly controlled by LD associated proteins, such as perilipin (PLIN) families[29]. Among these proteins, FITM1 is essential for the packaging of TG derived from endoplasmic reticulum (ER) and following initiation of LD formation, and PLIN5 sequesters TG from lipolysis by controlling the access of lipase and co-factors to LDs[30,31]. SSa was more potent in suppressing these genes and thus more efficient in regulating LD and TG degradation when compared with SSd. DAG played a critical role in the lipid homeostasis in the liver by serving as a central substrate for the production of not only monoacylglycerol (MAG), TG, and free FA, but also PC and PE, which are essential for the integrity and property of LD membrane (Fig. 4F)[32]. According to the lipidomic analysis, SSa and SSd shared similar capacities in relieving DAG accumulation in the liver and in regulating PC:PE levels (Supporting Information Fig. S7). However, SSd but not SSa, significantly upregulated the expression of genes implicated in the activation of glycerolipid, such as *Dgka*, *Dgkq*, and *Gk*, and genes involved in the following hydrolyzation of glycerolipid and release of FA, such as *Ces1d*, *Lipg*, and *Lipe*. PNPLA3 specifically catalyzes CoA-dependent acylation of 1-acyl-*sn*-glycerol 3-phosphate (LPA) to generate PA, the critical precursor of DAG and other glycerolipids. In addition, PNPLA3 possesses TG lipase activities and thus is involved in the regulation of LD and TG elimination. It has been well characterized that catalytically defective forms of PNPLA3, due to mutations (I148M), are strongly associated with NAFLD[33]. Most recently, by designing a ubiquitylation-resistant wild type PNPLA3, Linden et al.[34,35] further demonstrated that the accumulation of PNPLA3 on LD, but not defective enzymatic activity, resulted in hepatic steatosis, which suggested that suppressing the expression of PNPLA3 or promoting its clearance might serve as potential therapeutic targets for NAFLD. Our current study revealed that both SSa and SSd remarkably inhibited the transcription of *Pnpla3*, which was associated with the reduced PA levels in the liver. These results suggested that the lipid-lowering effects of SSa and SSd were also probably attributed to the regulation of *Pnpla3*. However, further studies are still required to investigate whether SSs alleviate PNPLA3 accumulation on LDs.

Meanwhile, SSa and SSd substantially modulated intrahepatic FA metabolism, including suppressing lipogenesis and promoting FA oxidation, and thus protected against lipotoxicity. Our study showed that SSa and SSd inhibited the maturation of SREBP-1 in a dose-dependent manner without suppressing transcription, suggesting the effects of SSs on SREBP-1 were post-translational and probably indirect. SSs may also hamper lipogenesis by modulating the interactions between SREBP-1 and other energy-sensing TFs. CEBPA and ChREBP (encoded by *Mlxipl*) are critical players in regulating both glucogenesis and lipogenesis, and both synergize with SREBP-1c in transcriptionally activating lipogenic genes[36–38]. Interestingly, SSs significantly reduced the mRNA levels of both *Cebpa* and *Mlxipl*. It would be of great interest to investigate the effects of SSs on the cleavage-dependent activation of SREBP and the interactions between SREBP-1c, CEBPA, and ChREBP. The effects of SSs on lipogenesis were only supported by RNA-sequencing, whereas the promotive effects of SSs on FA degradation were supported by both lipidomic and transcriptomic studies (Fig. 6F). Specifically, SSs significantly induced the expression of genes implicated in the transportation of FA, such as *Slc27a1* and *Abcd1*, which might facilitate the uptake of FA by either mitochondria and peroxisome, where FA was catabolized for energy production[39,40]. *Acox1* and *Acox3* were all essential genes involved in the degradation of VLCFA into FA with shorter chain[41]. SSa and SSd enhanced the transcription of *Acox1* and *Acox3* and thus reduced VLCFA and VLCFA-derived ACARs in the liver (Fig. 6E). Following ACSLs- and ACSMs-mediated transformation of FA into their active form acyl-CoA, CPT-1α, the rate-limiting enzyme, catalyzed the formation of ACARs that licensed the β-oxidation of FA in the mitochondria. The dramatically increased intracellular ACARs levels (about 10-fold) and significantly upregulated expression of these above genes strongly suggested that SSa and SSd were promising and potent modulators in facilitating FA degradation. Of note, SSd was more efficient in promoting FA clearance when compared to SSa, as illustrated by higher mRNA levels of genes and higher ACAR levels. Intriguingly, malonyl-CoA produced by ACCα (encoded by *Acaca*) in response to the accumulation of Acetyl-CoA, the subsequent product of FA β-oxidation, is a potential antagonist for the

enzymatic activity of CPT-1α and serve as a negative feedback mechanism[42,43]. SSs suppressed the expression of *Acaca*, which might inhibit the synthesis of malonyl-CoA and abrogate the feedback mechanism, and thus further strengthen the promotive effects of SSs on FA catabolism. These results suggested that SSs coordinately modulated both FA biogenesis and degradation and subsequently protected mice from NAFLD.

It is noteworthy that both SSa and SSd modulated gene expression on a large scale, indicated that upstream TFs were involved. By applying bioinformatic approaches and molecular simulation, we preliminarily identified that several TFs were potential molecular targets of SSa, SSd, and their metabolites. Among these TFs, PPARα was a master regulator of FA metabolism in hepatocytes, and RNA-seq results demonstrated that not only PPARα but also its co-activators were upregulated by SSs (Fig. 8F−H)[7,44]. The expression profile of PPARα target genes and molecular docking further supported that SSs relived NAFLD by, at least partly, acting as PPARα agonists. RXRα/PPARα heterodimer has been characterized as essential for the transcriptional activity of PPARα, and our results showed that SSs also upregulated the expression of RXRα at both mRNA and protein levels[45,46]. The downstream genes of RXRα were also upregulated in SSs-treated groups, including ATP-binding cassette sub-family G member proteins (ABCGs) and other genes involved in cholesterol metabolism (data not shown), suggesting potential therapeutic effects of SSa and SSd in cholesterol-related diseases, especially NALFD-associated cardiovascular complications[47]. Paradoxically, SSs also upregulated LXRα (encoded by *Nr1h3*), a nuclear receptor that has been established as a lipogenic TFs by interacting with SREBP-1c. SSs might also directly bind to LXRα as predicted by molecular docking[48−50]. More experimental evidence is urgently required to elucidate the complex interaction between SSs-mediated regulation of TFs. Furthermore, the molecular simulation indicated that various SSa and SSd metabolites, including SGh and SGd possessed similar or even stronger potencies in interacting with critical lipid metabolism-related TFs. These results encouraged systemic exploration of SS-, SS metabolite-, and SS derivative-induced anti-steatosis effects.

5. Conclusions

The current study systemically demonstrated that SSa and SSd, major bioactive ingredients derived from the most frequently used herbal medicine in liver diseases, significantly ameliorated hepatic steatosis and improved liver injury in an HFSW-fed NAFLD mouse model and OA:PA-treated primary hepatocytes. Integrative lipidomic and transcriptomic analysis revealed that SSa and SSd prevented glycerolipid accumulation, inhibited FA biosynthesis, promoted FA degradation, and subsequently recovered hepatic lipid homeostasis by broadly regulating TF-dependent gene expression. Our study not only sheds novel light on the complicated mechanisms underlying the anti-steatosis activities of widely used herbal medicine RB but also provides critical evidence inspiring the discovery and development of innovative therapeutic agents based on SSa and SSd for the treatment of NAFLD and related complications.

Acknowledgments

This work was supported by grants from the National Natural Science Foundation of China (Nos. 81773997 and 81073148 to Rong Sun; No. 82004029 to Runping Liu; No. 82004045 to Xiaojiaoyang Li) and Beijing University of Chinese Medicine (No. 2020-JYB-ZDGG-038 to Runping Liu, China). Runping Liu and Xiaojiaoyang Li are supported by grants from Beijing Nova Program of Science & Technology (Nos. Z201100006820025 and Z191100001119088, China). Rong Sun is supported by research fund 'Traditional Chinese medicine pharmacology and toxicology expert (No. ts201511107)' from the Taishan Scholar Project of Shandong Province (China).

Author contributions

Runping Liu, Rong Sun, and Xiaojiaoyang Li conceived the original idea and supervised the study. Junde Ge, Yajing Li, Qi Zheng, Qi Han, Yiqing Gu, and Yunqian Li conducted all the experiments. Runping Liu, Xiaojiaoyang Li, Nana Huang, and Yajie Cai performed data analysis. Runping Liu and Xiaojiaoyang Li prepared the manuscript and figures. All authors have approved the final manuscript.

Conflicts of interest

The authors have no conflicts of interest to declare.

Appendix A. Supporting information

Supporting data to this article can be found online at https://doi.org/10.1016/j.apsb.2021.03.018.

References

1. Brunt EM, Kleiner DE, Carpenter DH, Rinella M, Harrison SA, Loomba R, et al. NAFLD: reporting histologic findings in clinical practice. *Hepatology* 2021;**73**:2028−38.
2. Wegermann K, Suzuki A, Mavis AM, Abdelmalek MF, Diehl AM, Moylan CA. Tackling nonalcoholic fatty liver disease: three targeted populations. *Hepatology* 2021;**73**:1199−206.
3. Shiha G, Korenjak M, Eskridge W, Casanovas T, Velez-Moller P, Hogstrom S, et al. Redefining fatty liver disease: an international patient perspective. *Lancet Gastroenterol Hepatol* 2021;**6**:73−9.
4. Sheka AC, Adeyi O, Thompson J, Hameed B, Crawford PA, Ikramuddin S. Nonalcoholic steatohepatitis: a review. *J Am Med Assoc* 2020;**323**:1175−83.
5. Dhanasekaran R, Felsher DW. A tale of two complications of obesity: NASH and hepatocellular carcinoma. *Hepatology* 2019;**70**:1056−8.
6. Black D, Brockbank S, Cruwys S, Goldenstein K, Hein P, Humphries B. The future R&D landscape in non-alcoholic steatohepatitis (NASH). *Drug Discov Today* 2019;**24**:560−6.
7. Gross B, Pawlak M, Lefebvre P, Staels B. PPARs in obesity-induced T2DM, dyslipidaemia and NAFLD. *Nat Rev Endocrinol* 2017;**13**:36−49.
8. Francque S, Szabo G, Abdelmalek MF, Byrne CD, Cusi K, Dufour JF, et al. Nonalcoholic steatohepatitis: the role of peroxisome proliferator-activated receptors. *Nat Rev Gastroenterol Hepatol* 2021;**18**:24−39.
9. Lefere S, Puengel T, Hundertmark J, Penners C, Frank AK, Guillot A, et al. Differential effects of selective- and pan-PPAR agonists on experimental steatohepatitis and hepatic macrophages. *J Hepatol* 2020;**73**:757−70.
10. Rotman Y, Sanyal AJ. Current and upcoming pharmacotherapy for non-alcoholic fatty liver disease. *Gut* 2017;**66**:180−90.
11. Ratziu V, Harrison SA, Francque S, Bedossa P, Lehert P, Serfaty L, et al. Elafibranor, an agonist of the peroxisome proliferator-activated receptor-alpha and -delta, induces resolution of nonalcoholic

steatohepatitis without fibrosis worsening. *Gastroenterology* 2016; **150**:1147−59.e5.
12. Sumida Y, Yoneda M. Current and future pharmacological therapies for NAFLD/NASH. *J Gastroenterol* 2018;**53**:362−76.
13. Younossi ZM, Ratziu V, Loomba R, Rinella M, Anstee QM, Goodman Z, et al. Obeticholic acid for the treatment of non-alcoholic steatohepatitis: interim analysis from a multicentre, randomised, placebo-controlled phase 3 trial. *Lancet* 2019;**394**:2184−96.
14. Neuschwander-Tetri BA, Loomba R, Sanyal AJ, Lavine JE, Van Natta ML, Abdelmalek MF, et al. Farnesoid X nuclear receptor ligand obeticholic acid for non-cirrhotic, non-alcoholic steatohepatitis (FLINT): a multicentre, randomised, placebo-controlled trial. *Lancet* 2015;**385**:956−65.
15. Newsome PN, Palmer M, Freilich B, Sheikh MY, Sheikh A, Sarles H, et al. Volixibat in adults with non-alcoholic steatohepatitis: 24-week interim analysis from a randomized, phase II study. *J Hepatol* 2020; **73**:231−40.
16. Gao H, Yao XS. Strengthen the research on the medicinal and edible substances to advance the development of the comprehensive healthcare industry of TCMs. *Chin J Nat Med* 2019;**17**:1−2.
17. Wang YX, Du Y, Liu XF, Yang FX, Wu X, Tan L, et al. A hepatoprotection study of Radix Bupleuri on acetaminophen-induced liver injury based on CYP450 inhibition. *Chin J Nat Med* 2019;**17**:517−24.
18. Li X, Li X, Huang N, Liu R, Sun R. A comprehensive review and perspectives on pharmacology and toxicology of saikosaponins. *Phytomedicine* 2018;**50**:73−87.
19. Li X, Li X, Lu J, Huang Y, Lv L, Luan Y, et al. Saikosaponins induced hepatotoxicity in mice *via* lipid metabolism dysregulation and oxidative stress: a proteomic study. *BMC Complement Altern Med* 2017;**17**:219.
20. Asgharpour A, Cazanave SC, Pacana T, Seneshaw M, Vincent R, Banini BA, et al. A diet-induced animal model of non-alcoholic fatty liver disease and hepatocellular cancer. *J Hepatol* 2016;**65**: 579−88.
21. Keenan AB, Torre D, Lachmann A, Leong AK, Wojciechowicz ML, Utti V, et al. ChEA3: transcription factor enrichment analysis by orthogonal omics integration. *Nucleic Acids Res* 2019;**47**:W212−24.
22. Liu R, Li X, Zhu W, Wang Y, Zhao D, Wang X, et al. Cholangiocyte-derived exosomal long noncoding RNA H19 promotes hepatic stellate cell activation and cholestatic liver fibrosis. *Hepatology* 2019;**70**:1317−35.
23. Zechner R, Zimmermann R, Eichmann TO, Kohlwein SD, Haemmerle G, Lass A, et al. FAT SIGNALS—lipases and lipolysis in lipid metabolism and signaling. *Cell Metab* 2012;**15**:279−91.
24. Han J, Li E, Chen L, Zhang Y, Wei F, Liu J, et al. The CREB coactivator CRTC2 controls hepatic lipid metabolism by regulating SREBP1. *Nature* 2015;**524**:243−6.
25. Xu D, Wang Z, Xia Y, Shao F, Xia W, Wei Y, et al. The gluconeogenic enzyme PCK1 phosphorylates INSIG1/2 for lipogenesis. *Nature* 2020; **580**:530−5.
26. Joseph SB, Laffitte BA, Patel PH, Watson MA, Matsukuma KE, Walczak R, et al. Direct and indirect mechanisms for regulation of fatty acid synthase gene expression by liver X receptors. *J Biol Chem* 2002;**277**:11019−25.
27. Mottillo EP, Zhang H, Yang A, Zhou L, Granneman JG. Genetically-encoded sensors to detect fatty acid production and trafficking. *Mol Metab* 2019;**29**:55−64.
28. Brunmeir R, Xu F. Functional regulation of PPARs through post-translational modifications. *Int J Mol Sci* 2018;**19**:1738.
29. Gluchowski NL, Becuwe M, Walther TC, Farese RV Jr. Lipid droplets and liver disease: from basic biology to clinical implications. *Nat Rev Gastroenterol Hepatol* 2017;**14**:343−55.
30. Sztalryd C, Brasaemle DL. The perilipin family of lipid droplet proteins: gatekeepers of intracellular lipolysis. *Biochim Biophys Acta Mol Cell Biol Lipids* 2017;**1862**:1221−32.
31. de la Rosa Rodriguez MA, Kersten S. Regulation of lipid droplet-associated proteins by peroxisome proliferator-activated receptors. *Biochim Biophys Acta Mol Cell Biol Lipids* 2017;**1862**:1212−20.
32. Caillon L, Nieto V, Gehan P, Omrane M, Rodriguez N, Monticelli L, et al. Triacylglycerols sequester monotopic membrane proteins to lipid droplets. *Nat Commun* 2020;**11**:3944.
33. Trepo E, Valenti L. Update on NAFLD genetics: from new variants to the clinic. *J Hepatol* 2020;**72**:1196−209.
34. Linden D, Ahnmark A, Pingitore P, Ciociola E, Ahlstedt I, Andreasson AC, et al. *Pnpla3* silencing with antisense oligonucleotides ameliorates nonalcoholic steatohepatitis and fibrosis in *Pnpla3* I148M knock-in mice. *Mol Metab* 2019;**22**:49−61.
35. BasuRay S, Wang Y, Smagris E, Cohen JC, Hobbs HH. Accumulation of PNPLA3 on lipid droplets is the basis of associated hepatic steatosis. *Proc Natl Acad Sci U S A* 2019;**116**:9521−6.
36. Satoh S, Onomura D, Ueda Y, Dansako H, Honda M, Kaneko S, et al. Ribavirin-induced down-regulation of CCAAT/enhancer-binding protein alpha leads to suppression of lipogenesis. *Biochem J* 2019;**476**: 137−49.
37. Linden AG, Li S, Choi HY, Fang F, Fukasawa M, Uyeda K, et al. Interplay between ChREBP and SREBP-1c coordinates postprandial glycolysis and lipogenesis in livers of mice. *J Lipid Res* 2018;**59**: 475−87.
38. Abdul-Wahed A, Guilmeau S, Postic C. Sweet sixteenth for ChREBP: established roles and future goals. *Cell Metab* 2017;**26**:324−41.
39. Wiesinger C, Kunze M, Regelsberger G, Forss-Petter S, Berger J. Impaired very long-chain acyl-CoA beta-oxidation in human X-linked adrenoleukodystrophy fibroblasts is a direct consequence of ABCD1 transporter dysfunction. *J Biol Chem* 2013;**288**:19269−79.
40. Arif A, Terenzi F, Potdar AA, Jia J, Sacks J, China A, et al. EPRS is a critical mTORC1-S6K1 effector that influences adiposity in mice. *Nature* 2017;**542**:357−61.
41. Moreno-Fernandez ME, Giles DA, Stankiewicz TE, Sheridan R, Karns R, Cappelletti M, et al. Peroxisomal beta-oxidation regulates whole body metabolism, inflammatory vigor, and pathogenesis of nonalcoholic fatty liver disease. *JCI Insight* 2018;**3**:e93626.
42. Foster DW. Malonyl-CoA: the regulator of fatty acid synthesis and oxidation. *J Clin Invest* 2012;**122**:1958−9.
43. Schlaepfer IR, Joshi M. CPT1A-mediated fat oxidation, mechanisms, and therapeutic potential. *Endocrinology* 2020;**161**:bqz046.
44. Montagner A, Polizzi A, Fouche E, Ducheix S, Lippi Y, Lasserre F, et al. Liver PPARalpha is crucial for whole-body fatty acid homeostasis and is protective against NAFLD. *Gut* 2016;**65**:1202−14.
45. Plutzky J. The PPAR-RXR transcriptional complex in the vasculature: energy in the balance. *Circ Res* 2011;**108**:1002−16.
46. Nakamura MT, Yudell BE, Loor JJ. Regulation of energy metabolism by long-chain fatty acids. *Prog Lipid Res* 2014;**53**:124−44.
47. He C, Hu X, Weston TA, Jung RS, Sandhu J, Huang S, et al. Macrophages release plasma membrane-derived particles rich in accessible cholesterol. *Proc Natl Acad Sci U S A* 2018;**115**:E8499−508.
48. Zhao XY, Xiong X, Liu T, Mi L, Peng X, Rui C, et al. Long noncoding RNA licensing of obesity-linked hepatic lipogenesis and NAFLD pathogenesis. *Nat Commun* 2018;**9**:2986.
49. Xu P, Zhai Y, Wang J. The role of PPAR and its cross-talk with CAR and LXR in obesity and atherosclerosis. *Int J Mol Sci* 2018; **19**:1260.
50. Wang B, Tontonoz P. Liver X receptors in lipid signalling and membrane homeostasis. *Nat Rev Endocrinol* 2018;**14**:452−63.